

N-TYPE AND P-TYPE SILICON FOILS FABRICATED IN A QUASI-INLINE EPI REACTOR WITH BULK LIFETIMES EXCEEDING 500 μ s

S. Janz*, N. Milenković*, M. Drießen*, S. Reber†

*Fraunhofer Institute for Solar Energy Systems, Heidenhofstrasse 2, 79110 Freiburg, Germany

†Now with NexWafe GmbH, Hans-Bunte Strasse 19, 79108 Freiburg, Germany

ABSTRACT: In this publication we present free standing p- and n-type Si layers with thicknesses between 40 μ m (Epi foils) and 150 μ m (Epi Wafers) produced with epitaxy on electrochemically etched porous Si layers followed by mechanical lift-off. We show that reorganization and epitaxy in our quasi-inline tool leads to Si layers with very good crystal quality (etch pit density around 1000 cm^{-2}) and low contamination levels (interstitial Fe concentration around 10^{10}cm^{-3}). Thin p-type foils with just 40 μ m thickness show minority carrier lifetimes of up to 80 μ s mainly limited by the high dopant concentration of $5 \times 10^{16} \text{cm}^{-3}$. The n-type epitaxial wafers with 150 μ m thickness reach average minority carrier lifetimes of more than 1.5 ms. Appearing inhomogeneities of minority carrier lifetimes over the sample area are found to be due to surface cleaning process but not bulk quality related issues. The excellent lifetimes together with the very constant dopant concentration of our Si layers is sufficient for high efficiency solar cell architectures and a conversion efficiency of 20 % can be exceeded [1].

Keywords: CVD Based Deposition, Epitaxy, High Deposition Rate, Porous Silicon

1 INTRODUCTION

Lift-off technologies for semiconductor materials are well established in microelectronic production. However, although several groups are working on Si lift-off technologies for solar cell application [2, 3] up-scaling and throughput enhancement especially for the porosification and the epitaxy process have still to be proven before mass production can be launched. At Fraunhofer ISE we have been focusing on inline solutions and developed an Atmospheric Pressure Chemical Vapor Deposition (APCVD) tool called ProConCVD [4] which enables us to provide cost efficient reorganization and Si epitaxy processes which are the key for almost all lift-off concepts. For significant process adaptations like switching from p-type to n-type base doping we use the RTCVD 160 [5] furnace which is a quasi-inline but much more flexible tool. In this paper we present free standing Si layers of 40 μ m (Si foils) to 150 μ m (Epi Wafer) thickness with p- and n-type base doping with excellent electrical quality. Besides that, experiments using a new gas mixture setup are presented which enable a wide range of doping levels and an excellent reproducibility of the processes.

2 EXPERIMENTAL

The porosified 6-inch Cz samples for all experiments have been purchased at the Institute for Microelectronics in Stuttgart (IMS) featuring a low porosity layer on top of two high porosity layers. All wafers were cut down to 10 cm on one side and were etched in hydrofluoric acid (HF) with a concentration of 1 % before mounting in the quasi-inline RTCVD 160 furnace. The reorganization processes took place at 1150 °C under 100 % hydrogen atmosphere for up to 30 min at peak temperature. Subsequently the Si epitaxy process was done at the same temperature and in a trichlorosilane (TCS)/ H_2 atmosphere with a Cl/H gas flow ratio of 10 % and process times of about 50 to 120 min. As a reference substrate for epitaxial layer quality characterization we used $10 \times 10 \text{cm}^2$ Cz material. For the p-type samples the B_2H_6 flow was set to achieve a constant layer doping of approximately $5 \times 10^{16} \text{cm}^{-3}$. For the n-type samples we

adjusted our gas mixture system to be able to reach extremely low PH_3 flows. For the process development of n-type epitaxial layers in the range of $10^{13} - 10^{15} \text{cm}^{-3}$ we measured Spreading Resistance Profiles (SRP) on foils (40 μ m) as well as on Epi Wafers (150 μ m). Furthermore we used two different quartz inlays in the RTCVD tool for p and for n-type processing in order to minimize cross contaminations and to enable phosphorous dopant concentrations $< 10^{14} \text{cm}^{-3}$ and a reproducible process.

Prior to detachment mainly $4 \times 4 \text{cm}^2$ areas were defined on the wafers using a semi-automatic Nd:YAG-laser with a wavelength of 1064 nm (feed rate of 170 mm/s). We detached the foils in an in-house developed lifting tool which basically provides homogeneous soaking through special membrane materials over defined sample areas of up to $156 \times 156 \text{mm}^2$. Cross sections were prepared with simple sample breaking and investigated with Scanning Electron Microscopy (SEM).

Before scanning the surface with an optical microscope the samples were etched in SECCO¹ solution. From these images Stacking Fault Density (SFD) and Etch Pit Density (EPD) of the samples were derived using a software tool. The residual porous and highly doped Si layer was etched in a CP71 wet chemical bath with an etching rate of around 1.4 $\mu\text{m}/\text{min}$ for around 3 min. Both sides of all samples were passivated in an Atomic Layer Deposition (ALD) tool with 20 nm of Al_2O_3 . For the determination of iron, copper and oxygen we applied Glow Discharge Mass Spectroscopy (GDMS). Furthermore interstitial iron (Fe^i) was investigated on p-type foils with photoluminescence (PL) imaging [6]. Minority carrier lifetime measurements were done in a Quasi Steady State Photoconductance Decay (QSS-PC) tool from *Sinton instruments* and with a Microwave Photoconductance Decay tool *WT2000D* from *Semilab*.

3 RESULTS AND DISCUSSION

Area definition and lift-off for all layer thicknesses

¹ Secco-etch: $\text{HF} + \text{K}_2\text{Cr}_2\text{O}_7 + \text{H}_2\text{O}$ in a ratio of $\text{HF} : \text{H}_2\text{O} = 2 : 1$ with 44 g $\text{K}_2\text{Cr}_2\text{O}_7$ dissolved in 1 l of H_2O . It etches defects on all surfaces.

worked out proving the robustness of the whole process chain. However, it became apparent that the storage of the porosified samples has significant influence on the detachability yield of the epitaxial layers. Especially samples which had been stored for more than 1 month had to be cleaned in HF again before mounting in the RTCVD 160. This measure increased the lift-off yield again, however, in cross section images the structures look more hollowly. As the samples had enough time for native oxide formation during long time storage this effect can be explained by the additional Si removal with the second HF cleaning in comparison to samples cleaned just once.

Table 1: Etch pit density and stacking fault density of epitaxially grown Si layers with around 100 μm thickness.

Process	etch pit density [cm^{-2}]	stacking fault density [cm^{-2}]
Reorganization +Epi	≈ 1000	≈ 100
Epi on Cz Cz reference	≈ 1000	< 10

In Table 1 the etch pit and stacking fault densities of the epitaxial layers grown on the reorganized porous layer stacks and on the Cz reference are presented. We find that EPDs are in the same range of around 1000 cm^{-2} and that SFD are one order of magnitude higher (around 100 cm^{-2}) but still in a reasonable range for the porous templates.

3.1 P-type epitaxial layers

GDMS finds no Fe and Cu in the EpiWafers which means that the concentration is below the detection limit of around 10^{14} cm^{-3} . The oxygen concentration is in the range of 10^{16} cm^{-3} , however, due to the large surface (residual porous layer) of the samples the share of the bulk concentration is expected to be overestimated.

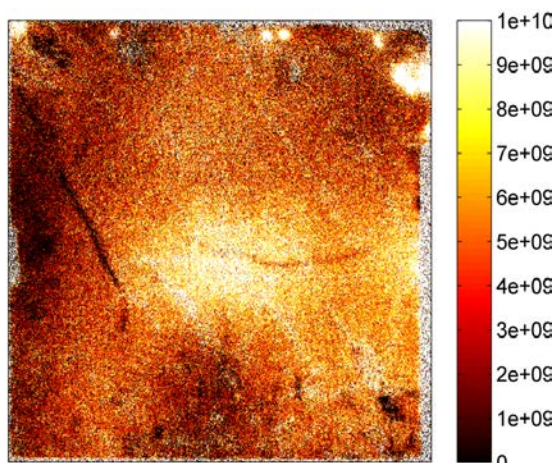


Figure 1: Interstitial Fe concentration determined by photoluminescence measurement on a $4 \times 4 \text{ cm}^2$ p-type EpiWafer.

On the same p-type samples PL-imaging (see Figure 1) finds interstitial iron concentrations of just 10^{10} cm^{-3} and below. As Fe is representative for many transition metals we can conclude that these Fe contaminations neither in the solved form nor in large

cluster, as they would be found with GDMS, are limiting the quality of our free standing epitaxial Si layers.

During etching of the free standing Si layers in CP71 the removal of one or two layers with a concentric progression from the edges to the center of the samples can be observed (porous side). As we know from SEM micrographs that the detachment process takes place in one of the highly porous layers it seems reasonable that the residual layer on the lifted layer is varying locally in thickness and surface structure. Especially when the detachment takes place in the upper highly porous layer a dense layer with an underlying porous layer remains on the surface. Inhomogeneous etching behavior is the consequence. Besides that we randomly find optical features after Al_2O_3 deposition which we think are connected to a surface contamination issue.

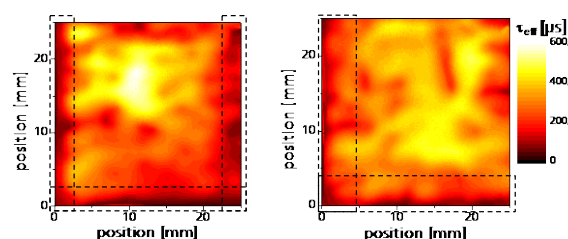


Figure 2: Microwave Photoconductance Decay measurement of two $100 \mu\text{m}$ thick silicon EpiWafers (n-type) etched in different carriers with rectangular (left) and with triangular (right) shape. The indicated areas (dashed frame) show the influence of carrier geometry on surface cleaning.

In parallel experiments we performed the CP71 cleaning on two samples from the same epitaxially grown and lifted layer but used a rectangular and a triangular shaped carrier, respectively. MWPCD measurements (see Figure 2) show on both samples large variations in effective minority carrier lifetime (τ_{eff}). Especially the regions where the samples were in contact with the carriers show significantly lower lifetime values. Although optically no difference can be found on the surface it is obvious that the etching process in and close to the carrier slots is different due to other mixing conditions of the chemicals. We conclude that deviations in surface structure as well as possible contamination and surface cleaning linked issues are the reason for the variations of the measured τ_{eff} values over the sample area.

In Figure 3 the MWPCD mapping of effective minority carrier lifetime for a $40 \mu\text{m}$ thin p-type Si foil is shown. Locally values of up to $80 \mu\text{s}$ can be measured. Although the average τ_{eff} measured with QSSPC is as high as $43 \mu\text{s}$ we still would expect higher lifetime values as transition metal contaminations are obviously not the reason for the overall bulk limitation.

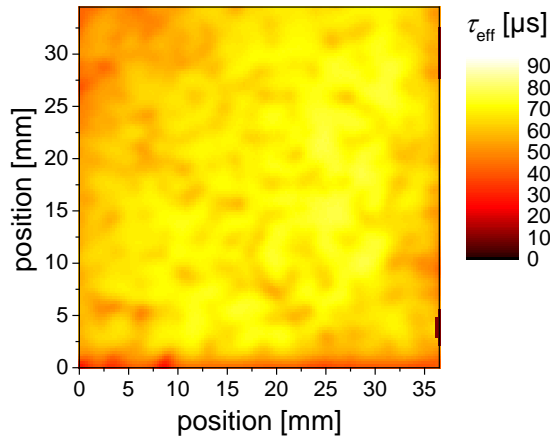


Figure 3: Microwave Photoconductance Decay measurement of p-type Epi foil with a thickness of 40 μm .

It is well known, that the bulk lifetime is, due to Auger recombination, limited by doping concentration. Using the model of Richter *et al.* [7] one can calculate that τ_{bulk} is limited to 450 μs for a p-dopant concentration of $5 \times 10^{16} \text{ cm}^{-3}$.

Additionally, the measured effective carrier lifetime strongly depends on the surface recombination velocity, especially for a sample thickness lower than 100 μm . For a better understanding of the influence of surface recombination velocity (SRV) and bulk lifetime τ_{bulk} on the effective carrier lifetime τ_{eff} we consider the following equation from [8]

$$\frac{1}{\tau_{\text{eff}}} = \frac{1}{\tau_{\text{bulk}}} + \frac{1}{\frac{W^2}{\pi^2 \cdot D} + \frac{W}{2 \cdot S}}, \quad (1)$$

with τ_{bulk} being the bulk lifetime of the epitaxial Si layers, W being the thickness of the foil and S being the surface recombination velocity on front and rear side. When applying this equation to our p-type Si foils with a thickness of 40 μm and assuming a very good surface passivation of Al_2O_3 with $S = 3 \text{ cm/s}$ leads to a maximum possible τ_{eff} for our foils of 240 μs (1 sun illumination). Considering the surface issues discussed above we conclude that the maximum τ_{eff} values of 80 μs measured on our foils are already quite good. In order to approach the uncertainty of surface passivation quality on our samples we started still ongoing thickness variation experiments which will help us to clearly distinguish between surface and bulk limitations.

3.2 N-type epitaxial layers

In Figure 4 we present SRP measurements of epitaxially grown n-type Si layers. In green (dashed line) the complete profile for a thin layer still attached to the substrate can be found. The phosphorous doping level of around $2 \times 10^{16} \text{ cm}^{-3}$ slightly increases from surface to the p n-junction and then changes to boron levels of more than 10^{18} cm^{-3} in the seed wafer. After adaptation of the gas mixture system we established several epitaxy processes which cover the phosphorous doping range from around $3 \times 10^{13} \text{ cm}^{-3}$ to $5 \times 10^{15} \text{ cm}^{-3}$. The SRP measurements were done on thick layers with more than 100 μm . These representative samples proof the very constant doping level (blue, orange and red lines) over the top 30 μm .

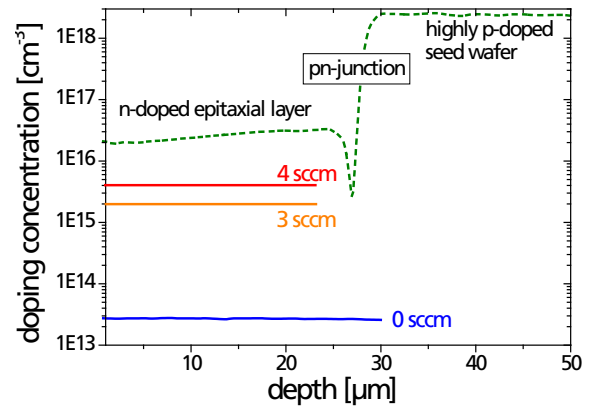


Figure 4: Spreading resistance profiling of epitaxially grown Si EpiWafers (n-type) at phosphine gas flows of 0 sccm (blue), 3 sccm (orange) and 4 sccm (red) as well as a complete profile for a still attached Si layer of 30 μm thickness. This measurement shows epitaxial layer and seed wafer (dashed).

As SRP measurements are limited to some extent to these layer thicknesses (for single measurement runs) we prepared additional samples close to the residual porous layer region which are not shown here. We find a small out-diffusion of boron from the seed wafer into the epitaxial layer but this is limited to several micrometers depth. As this region is anyway removed with the residual porous Si layer we can conclude that the doping profile is perfectly stable over the whole EpiWafer. As long as no other processes are performed with the same reactor inlay of the RTCVD tool cross-contaminations and memory effect can be neglected and reproducible processes can be ensured.

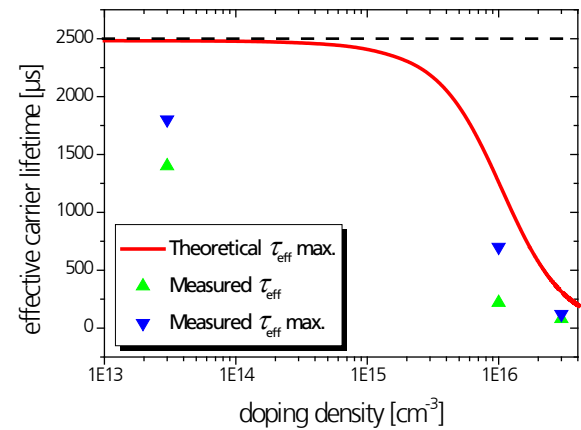


Figure 5: Effective minority carrier lifetimes calculated using equation (1) for a 150 μm thick EpiWafer with a passivated surface ($S_{\text{eff}}=3 \text{ cm/s}$) (red) compared to average (green triangular) and maximum (blue triangular upside down) values measured on EpiWafers with different dopant concentration.

In Figure 5 we present the calculated effective carrier lifetimes for a 150 μm thick EpiWafer with a perfectly well passivated surface with $S=3 \text{ cm/s}$ (red line). The measured mean (green triangular) and the maximum values (blue triangular) at the lowest possible and at doping levels in the range of 10^{16} cm^{-3} are already very close to theoretical values. Besides that they nicely follow the theoretical curve showing the dominating Auger limitation from dopant

levels of $5 \times 10^{15} \text{ cm}^{-3}$ on and higher.

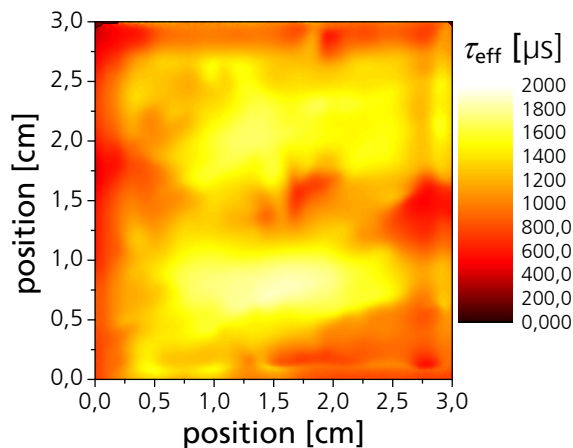


Figure 6: Microwave Photoconductance Decay measurement of n-type EpiWafer with a thickness of 150 μm .

In Figure 6 the MWPCD mapping of effective minority carrier lifetimes for a 150 μm thick n-type Si EpiWafer is shown. The average value for τ_{eff} measured with QSSPC is as high as 1.5 ms. Although the surface looks optically perfectly homogeneous again some lifetime variations over the area can be found. However, with lifetime maxima of over 1.8 ms the excellent electrical quality of the EpiWafers is proven beyond doubt.

4 CONCLUSIONS

In this publication we present free standing Si layers either p- or n-type in the thickness range between 40 and 150 μm . The reorganization and epitaxy process on porous seed wafers leads to very good crystal qualities with EPDs of 1000 cm^{-2} and SFD of 100 cm^{-2} . With GDMS and PL measurements we could show that there are no significant metal clusters and that the interstitial Fe concentration is 10^{10} cm^{-3} and below. Thin p-type foils with just 40 μm thickness show maximum minority carrier lifetimes of up to 80 μs limited by surface contamination issues and the high dopant concentration of $5 \times 10^{16} \text{ cm}^{-3}$ which theoretically does not allow more than $\tau_{\text{eff}} = 240 \mu\text{s}$ for this material. The n-type epitaxial wafers (EpiWafer) with 150 μm thickness reach average minority carrier lifetimes of more than 1.5 ms. With the introduced adaptations in our gas mixture system we are able to provide such high quality layers with very constant dopant concentrations from $3 \times 10^{13} \text{ cm}^{-3}$ to $5 \times 10^{15} \text{ cm}^{-3}$. Therefore we are confident that our material is appropriate for high efficiency solar cell concepts.

5 ACKNOWLEDGEMENTS

The authors would like to express their gratitude to Harald Lautenschlager, Mira Kwiatkowska, Elke Gust, Kai Schillinger, Michaela Winterhalder, Bernd Steinhäuser, Antonio Leimenstoll, Felix Schätzle and Nadine Weber at ISE for their support and input in many valuable discussions. This work was funded by the German Federal Ministry for the Environment, Nature Conservation and Nuclear Safety (Contract Number FKZ 0325199A).

6 REFERENCES

- [1] G. P. Willeke *et al.*, *Thin crystalline silicon solar cells*, Solar Energy Materials & Solar Cells 72 (2002) pp. 191–200.
- [2] J. H. Petermann *et al.*, *19%-efficient and 43 μm -thick crystalline Si solar cell from layer transfer using porous silicon*, Progress in Photovoltaics: Research and Applications, 2012. 20(1) 1-5.
- [3] H.S. Radhakrishnan *et al.*, *Improving the Quality of Epitaxial Foils Produced Using a Porous Silicon-based Layer Transfer Process for High-Efficiency Thin-Film Crystalline Silicon Solar Cells*, Photovoltaics, IEEE Journal of, 2013. PP(99): p. 1-8.
- [4] S. Reber *et al.*, *Advances in equipment and process development for high-throughput continuous silicon epitaxy*, Proceedings of the 27th EUPVSEC, Frankfurt, Germany (2012) p. 2.
- [5] S. Reber *et al.*, *The RTCVD160 – a new Lab-Type Silicon CVD Processor for Silicon Deposition on Large Area Substrates*, Proceedings of the 19th EUPVSEC, Paris, France (2004).
- [6] D. McDonald *et al.*, *Imaging interstitial iron concentrations in boron-doped crystalline silicon using photoluminescence*, JAP 103, 073710 □(2008).
- [7] A. Richter, *et al. Improved quantitative description of Auger recombination in crystalline silicon*, DOI: 10.1103/PhysRevB.86.165202.
- [8] D. K. Schroder *et al.*, *Semiconductor Material and Device Characterization*, 1st ed., 1990, New York, John Wiley & Sons. p. 599.